

Supplementary Information**“Nuclear ADP-Ribosylation Drives IFN γ -dependent STAT1 α Enhancer Formation In Macrophages”**

Gupte et al. (2021)

This document contains the following supplementary information:

| | <u>Page</u> |
|---|-------------|
| • Supplementary Table 1. List of Primers used..... | 2 |
| • Supplementary Figure 1. PARP-1 Regulates IFN γ -driven gene expression in macrophages..... | 4 |
| • Supplementary Figure 2. PARP inhibition alters the IFN γ -dependent STAT1 α cistrome | 5 |
| • Supplementary Figure 3. Loss of PARP-1 leads to attenuation of STAT1 α phosphorylation at S727..... | 6 |
| • Supplementary Figure 4. Inhibition of ADP-ribosylation by PJ34 leads to a loss of STAT1 α phosphorylation at S727. | 8 |
| • Supplementary Figure 5. Identification of sites of ADP-ribosylation on STAT1 α by using mass spectrometry. | 10 |
| • Supplementary Figure 6. Ectopic expression of STAT1 α Wt and mutants in iBMDMs | 11 |
| • Supplementary Figure 7. IFN γ -dependent transcription in iBMDMs is regulated by ADP-ribosylation of STAT1 α | 12 |
| • Supplementary Figure 8. Site-specific ADPRylation of STAT1 α on its DBD and TA domain us required for pro-inflammatory responses in macrophages | 14 |
| • Supplementary Figure 9. Loss of site-specific ADP-ribosylation of the STAT1 α DBD results in enhanced binding to DNA. | 15 |
| • Supplementary Figure 10. Loss of site-specific ADP-ribosylation of the STAT1 α TA domain attenuates IFN γ -stimulated phosphorylation at S727..... | 17 |

Supplementary Table 1. List of Primers Used

| <i>Primers used for cloning the Flag-tagged STAT1α cDNA</i> | |
|---|---|
| Human STAT1 α Forward | 5'-ATGTCTCAGTGGTACGAACTTCAGCAGC-3' |
| Human STAT1 α Reverse | 5'- CTATACTGTGTTTCATCATACTGTTCGAA-3' |
| Mouse STAT1 α Forward | 5'ATGTCACAGTGGTTCGAGCTTCA-3' |
| Mouse STAT1 α Reverse | 5'-TTATACTGTGCTCATCATACTGTCAAATTCGGG-3' |

| <i>Primers used for mutagenizing the STAT1α cDNA</i> | |
|--|---|
| Human STAT1 α DBD Mutant (E393/4Q) Forward | 5'- GACTGCCATTGGTGGACTGCTGCATGTTTCATCACTTTTGT-3' |
| Human STAT1 α DBD Mutant (E393/4Q) Reverse | 5'- ACAAAGTGATGAACATGCAGCAGTCCACCAATGGCAGTC-3' |
| Human STAT1 α TA Mutant (D721N) Forward | 5'- GGAGCAGGTTGTTTGTGGTCTGAAGTCTAGAAGGG-3' |
| Human STAT1 α TA Mutant (D721N) Reverse | 5'- CCCTTCTAGACTTCAGACCACAAACAACCTGCTCC-3' |
| Mouse STAT1 α DBD Mutant E393/4Q Forward | 5'- CTGCCAGACTCCGTTGGTGGACTGCTGCATGTTTCATCACTTTTGTGTGC-3' |
| Mouse STAT1 α DBD Mutant E393/4Q Reverse | 5'-GCACACAAAAGTGATGAACATGCAGCAGTCCACCAACGGAAGTCTGGCAG-3' |
| Mouse STAT1 α TA Mutant (D721N) Forward | 5'- GAAGCAGGTTGTTTGTGGTCTGAAGTCTAGAAGGG-3' |
| Mouse STAT1 α TA Mutant (D721N) Reverse | 5'- CCCTTCTAGACTTCAGACCACAAACAACCTGCTTC-3' |

| <i>qPCR Primers</i> | |
|----------------------|------------------------------|
| <i>ccl7</i> Forward | 5'- CCCATCAGAAGTGGGTCGAG-3' |
| <i>ccl7</i> Reverse | 5'- TGCTTCTTGGCTCCTAGGTTG-3' |
| <i>cc12</i> Forward | 5'- GCTGACCCCAAGGAGAAGTG-3' |
| <i>ccl12</i> Reverse | 5'- TGGGGAACCTTCAGGGGGAAA-3' |

[See Supplementary Figure 1 on the next page]

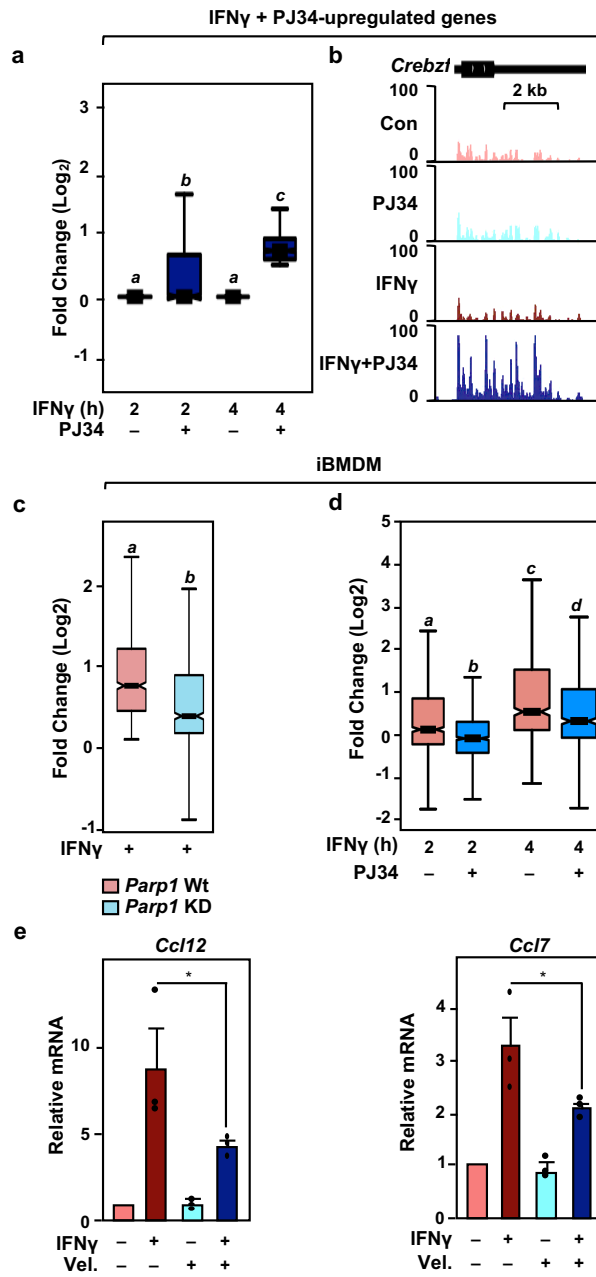
Supplementary Figure 1. PARP-1 Regulates IFN γ -driven gene expression in macrophages.

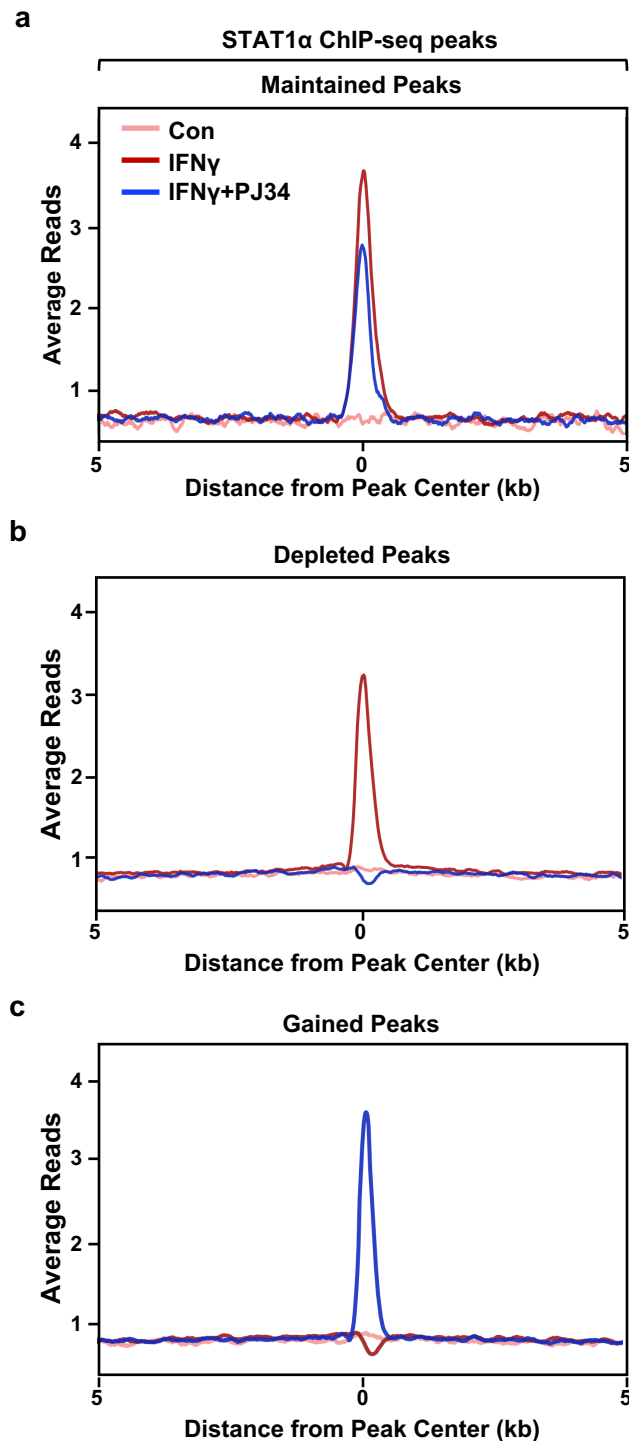
(a), (b) Expression of genes upregulated upon IFN γ treatment \pm PJ34 in BMDMs. (a) Box plots showing the fold change in expression. Boxes represent 25th – 75th percentile (line at median) with whiskers at 1.5*IQR. Boxes marked with different letters are significantly different from each other (Wilcoxon Signed-Rank test; $p < 2.2 \times 10^{-16}$). Box plots represent 845 genes. (b) RNA-seq browser tracks showing the expression of *Crebzf* in the corresponding treatment conditions.

(c), (d) PARP-1 catalytic activity is required for the modulation of IFN γ -dependent gene expression in iBMDMs. Wild-type (Wt) and *Parp1* knockdown (KD) iBMDMs were treated with IFN γ \pm PJ34 as indicated. Box plots showing the fold change in expression. Boxes represent 25th – 75th percentile (line at median) with whiskers at 1.5*IQR. Boxes marked with different letters are significantly different from each other (Wilcoxon Signed-Rank test; $p < 2.2 \times 10^{-16}$). Box plots represent 781 genes (c); 936 genes (2 h) and 665 genes (4 h) in (d).

(e) Experiments similar to those shown in (c) and (d). Bar graphs showing the relative mRNA levels upon treatment IFN γ treatment \pm Veliparib (Vel.). The p-values were determined using one-way ANOVA followed by Fisher's LSD test ($n = 3$; * = 0.0138 for *Ccl12*; * = 0.0116 for *Ccl7*).

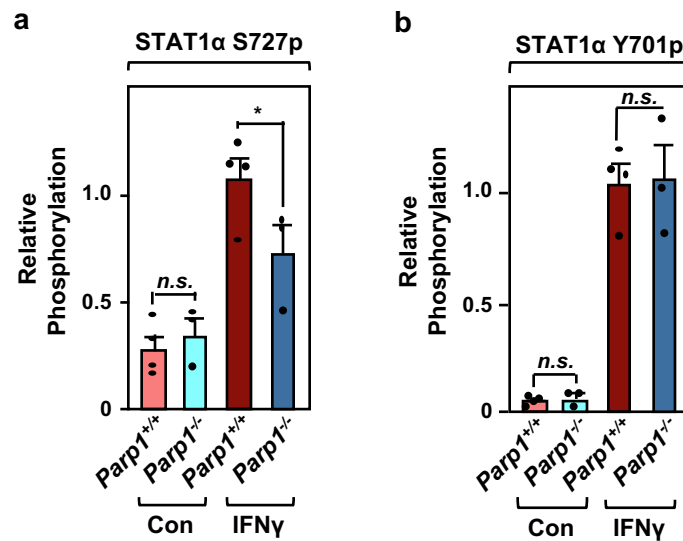
Supplementary Figure 1





Supplementary Figure 2. PARP inhibition alters the IFN γ -dependent STAT1 α cistrome.

Metaplots showing the read density within a 10 kb window surrounding the peak center for ‘maintained’ (a), ‘depleted’ (b) and ‘gained’ (c) STAT1 α peaks. ChIP-seq was performed on BMDMs as described in Figure 2.



Supplementary Figure 3. Loss of PARP-1 leads to attenuation of STAT1 α phosphorylation at S727.

(a), (b) Quantification of immunoblots ($n = 3$ or 4 as indicated) for STAT1 α S727p (a) and STAT1 α Y701p (b) relative to total STAT1 α levels. β -Tubulin loading was used as a normalization control. The p-values were determined using two-way ANOVA followed by Tukey's multiple comparison tests (n.s., not significant at $p < 0.05$; * = 0.0204). Error bars represent mean \pm SEM.

[See Supplementary Figure 4 on the next page]

Supplementary Figure 4. Inhibition of ADP-ribosylation by PJ34 leads to a loss of STAT1 α phosphorylation at S727.

(a) Inhibition of PARP-1 catalytic activity does not affect IFN γ -induced STAT1 α nuclear translocation. Immunofluorescent staining for STAT1 α was performed in BMDM treated with IFN γ (1 hour) \pm PJ34. The nuclei were visualized with DAPI staining. Scale bar: 10 μ m.

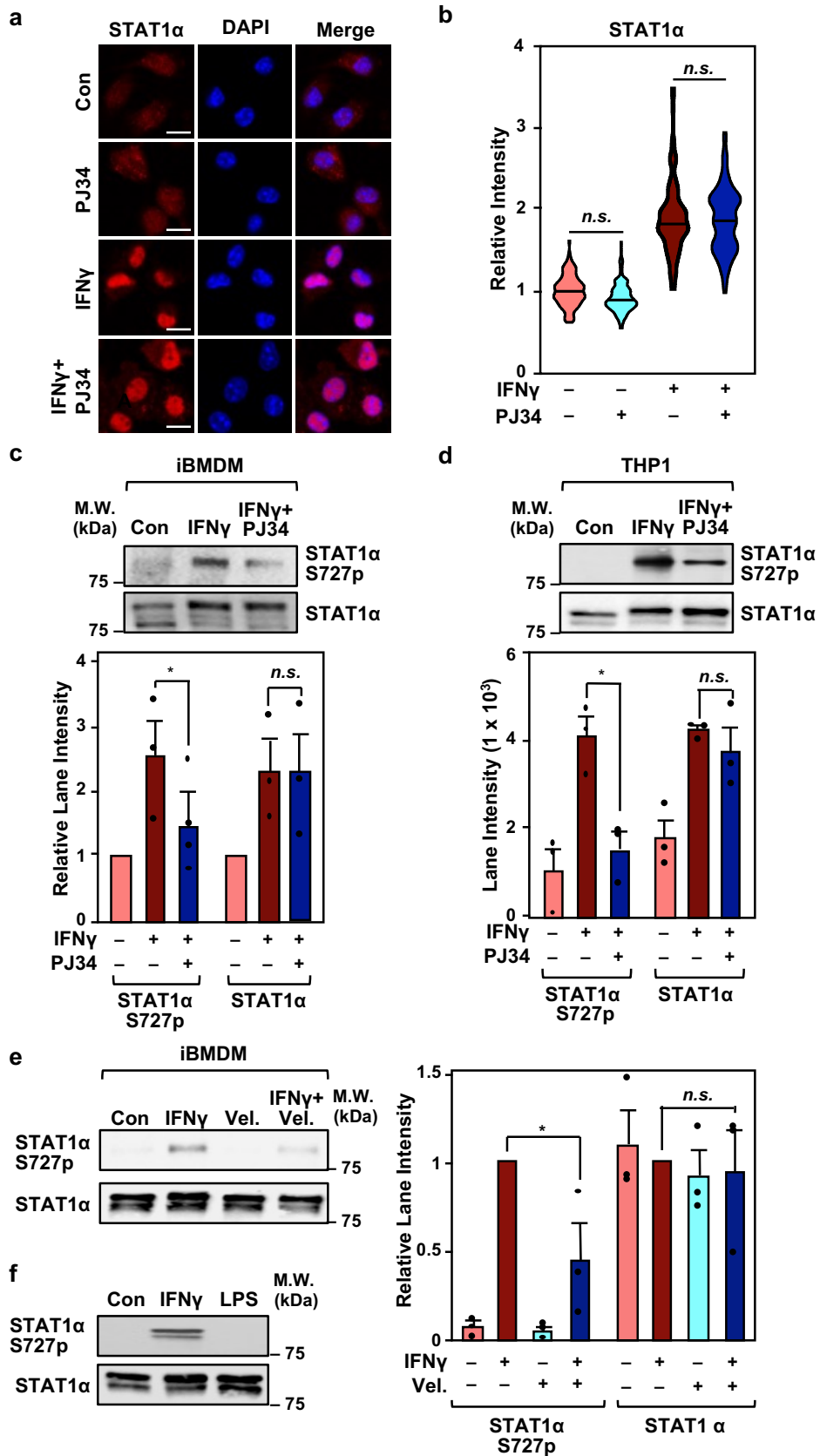
(b) Violin plots showing the quantification of immunofluorescent staining data from (A). The p-values were determined using one-way ANOVA followed by Tukey's multiple comparison tests (n.s., not significant at $p = 0.9791$).

(c), (d) Immunoblots for STAT1 α S727p in iBMDMs (c) and THP1 cells (d). Bottom panels show quantification of the immunoblots for 3 independent experiments. (c) The p-values were determined using paired, two-tailed Student's t-test (* = 0.0403; n.s. > 0.05). (d) The p-values were determined using two-way ANOVA followed by Tukey's multiple comparison tests (* = 0.0130; n.s. > 0.05). Error bars represent mean \pm SEM. Uncropped immunoblots are provided as a Source Data file.

(e) Immunoblots for STAT1 α S727p in iBMDMs treated with IFN γ \pm Veliparib (Vel.) as indicated. Right panel shows quantification of the immunoblots for 3 independent experiments. The p-values were determined using two-way ANOVA followed by Fisher's LSD tests (* = 0.0127; n.s. > 0.05). Error bars represent mean \pm SEM. Uncropped immunoblots are provided as a Source Data file.

(f) Immunoblots for STAT1 α S727p in iBMDMs treated with IFN γ or LPS as indicated. The immunoblots are representative of 2 independent experiments. Uncropped immunoblots are provided as a Source Data file.

Supplementary Figure 4



[See Supplementary Figure 5 on the next page]

Supplementary Figure 5. Identification of sites of ADP-ribosylation on STAT1 α by using mass spectrometry.

(a) STAT1 α is ADPRylated in IFN γ -treated iBMDMs. Immunoblots showing ADPRylation in iBMDMs expressing Flag-tagged STAT1 α and stimulated with IFN γ \pm PJ34. The ectopically expressed STAT1 α was immunoprecipitated from nuclear extracts using a Flag antibody. PAR levels were detected using an ADP-ribose detection reagent (AF1521-Fc reagent). The immunoblots are representative of 3 independent experiments. Uncropped immunoblots are provided as a Source Data file.

(b) Immunoblots showing ADPRylation of STAT1 α by PARP-1 in vitro from Fig. 4b. Molecular weight (M.W.) markers are used to show corresponding protein sizes in the top panel (PAR). Arrow indicates the band for ADPRylated STAT1 α . The immunoblots are representative of 3 independent experiments. Uncropped immunoblots are provided as a Source Data file.

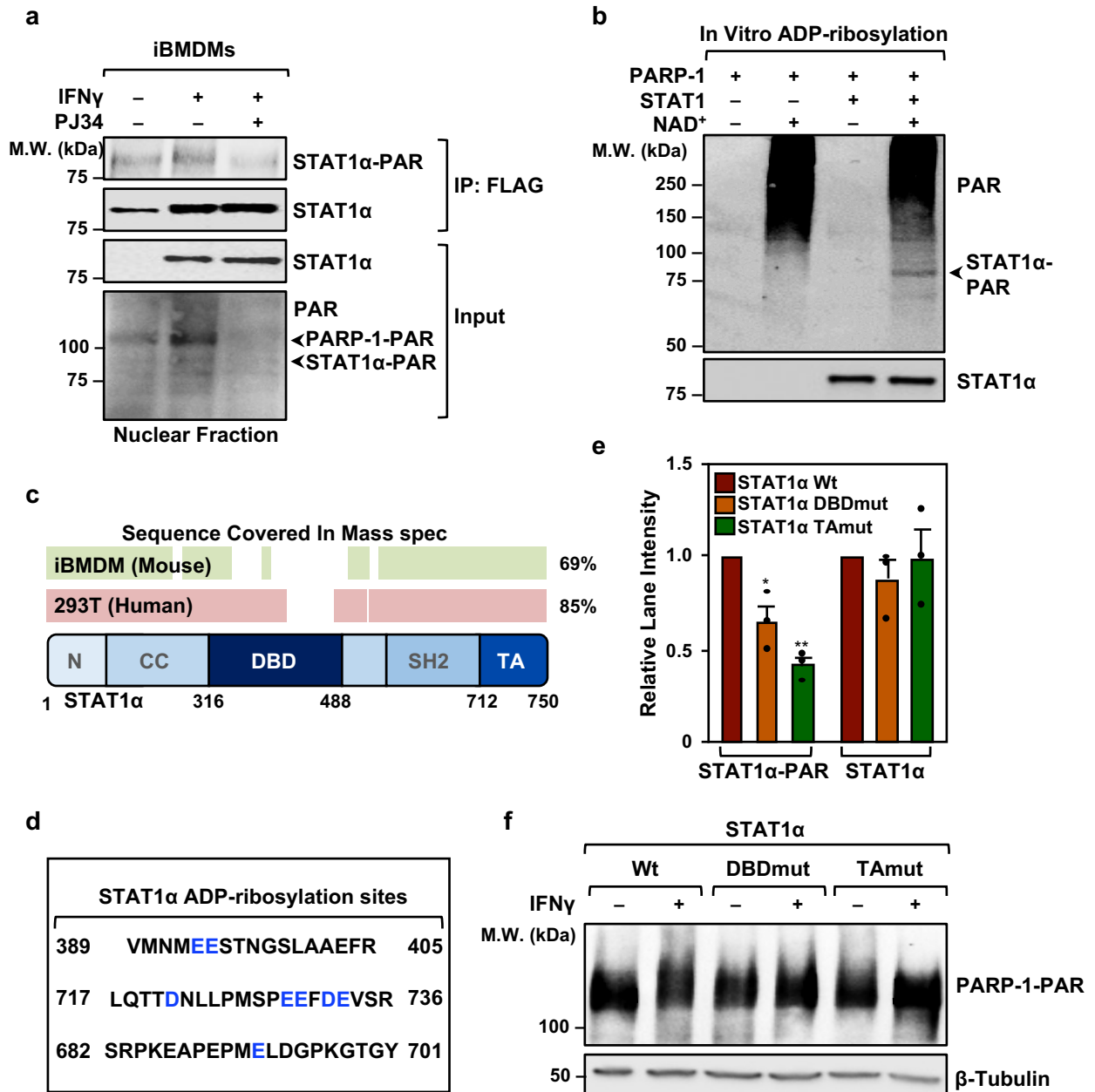
(c) *(Top)* Schematic diagram showing the protein coverage obtained from mass spectrometry assays of endogenous STAT1 α (iBMDMs) and ectopically expressed STAT1 α (293T cells). *(Bottom)* Schematic diagram of STAT1 α showing its functional domains, including the N-terminal (N), coiled-coil (CC), DNA binding (DBD), Src Homology 2 (SH2), and transactivation (TA) domains.

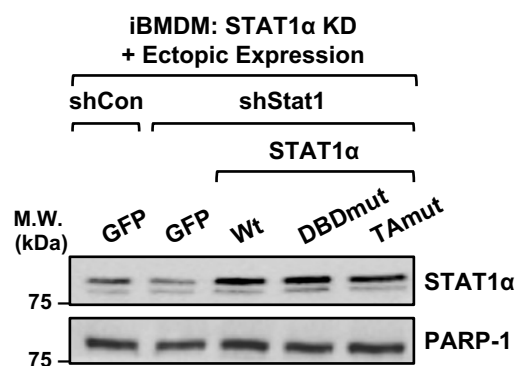
(d) The sites of ADP-ribosylation on STAT1 α on selected peptides determined by mass spectrometry.

(e) Quantification of immunoblots from Fig. 4e for 3 independent experiments (two-way ANOVA followed by Dunnett's multiple comparisons test; * = 0.022 , ** = 0.0006). Error bars represent mean \pm SEM.

(f) Immunoblots showing total ADPRylation in iBMDMs ectopically STAT1 α wildtype (Wt) or ADPRylation-defective mutants (DBDmut and TAmut). iBMDMs were stimulated with IFN γ as indicated. The immunoblots are representative of 3 independent experiments. Uncropped immunoblots are provided as a Source Data file.

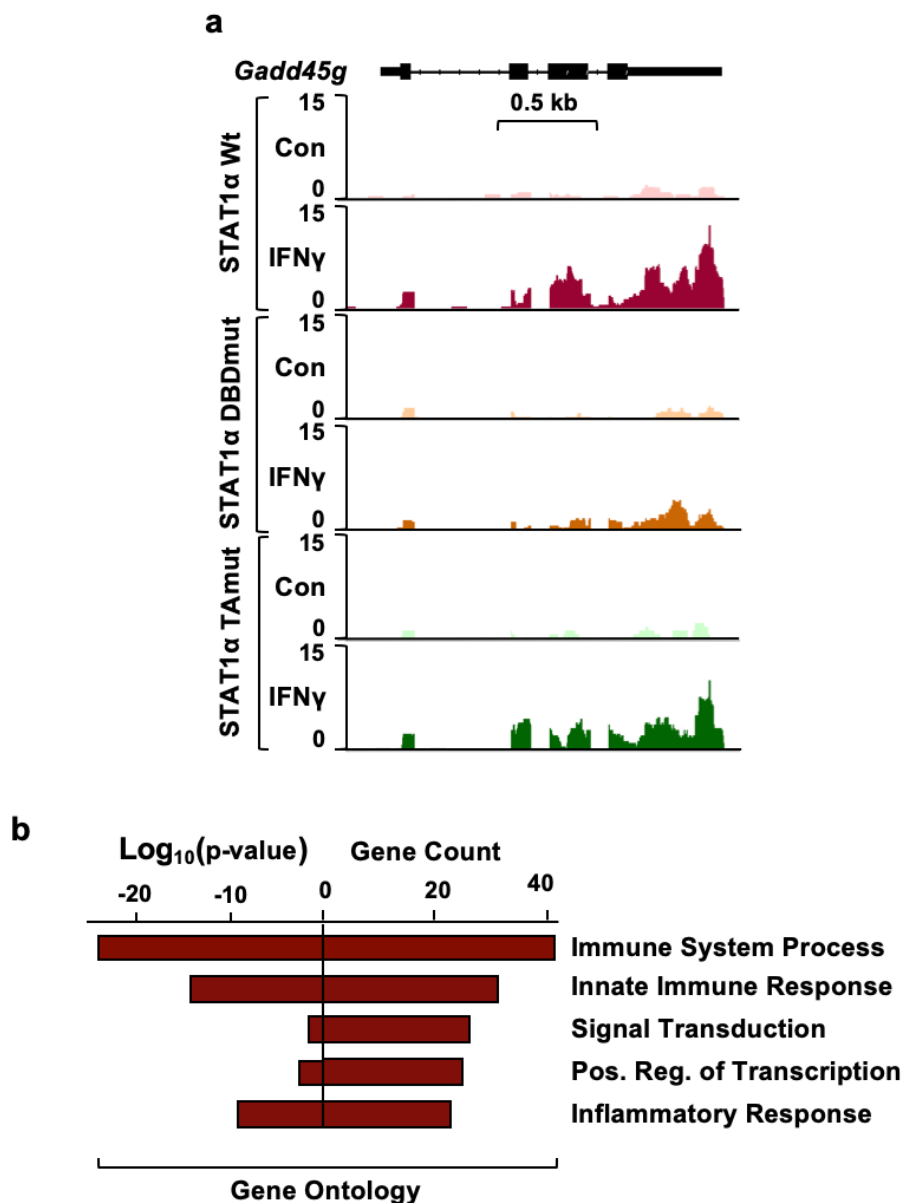
Supplementary Figure 5





Supplementary Figure 6. Ectopic expression of STAT1 α Wt and mutants in iBMDMs.

Immunoblots showing inducible ectopic expression of STAT1 α wild-type (Wt) and ADP-ribosylation site mutants (DBDmut and TAmut) in iBMDMs subjected to concurrent shRNA-mediated knockdown of endogenous STAT1 α (shStat1) or a control knockdown (shCon). The immunoblots are representative of 3 independent experiments. Uncropped immunoblots are provided as a Source Data file.



Supplementary Figure 7. IFN γ -dependent transcription in iBMDMs is regulated by ADP-ribosylation of STAT1 α .

(a) RNA-seq browser tracks showing IFN γ -induced gene expression at the indicated locus (*Gadd45g*). RNA-seq was performed in iBMDMs ectopically expressing Wt or ADP-ribosylation site mutants (DBDmut and TAMut) with concurrent shRNA-mediated knockdown of endogenous STAT1 α .

(b) Gene ontology analysis for IFN γ -stimulated genes that are dependent on STAT1 α ADP-ribosylation for proper expression. The gene counts in each term and the log₁₀(p-value) for each term are shown.

[See Supplementary Figure 8 on the next page]

Supplementary Figure 8. Site-specific ADPRylation of STAT1 α on its DBD and TA domain is required for pro-inflammatory responses in macrophages.

(a) Schematic diagram showing the role of site-specific ADPRylation of STAT1 α in downstream pro-inflammatory responses in macrophages.

(b) Quantification of phagocytosis showing the number of pHrodo⁺ cells relative to the total number of cells per field for 3 independent experiments (unpaired, two-tailed Student's t-test; ** = 0.0019, *** = 0.0007). Error bars represent mean \pm SEM.

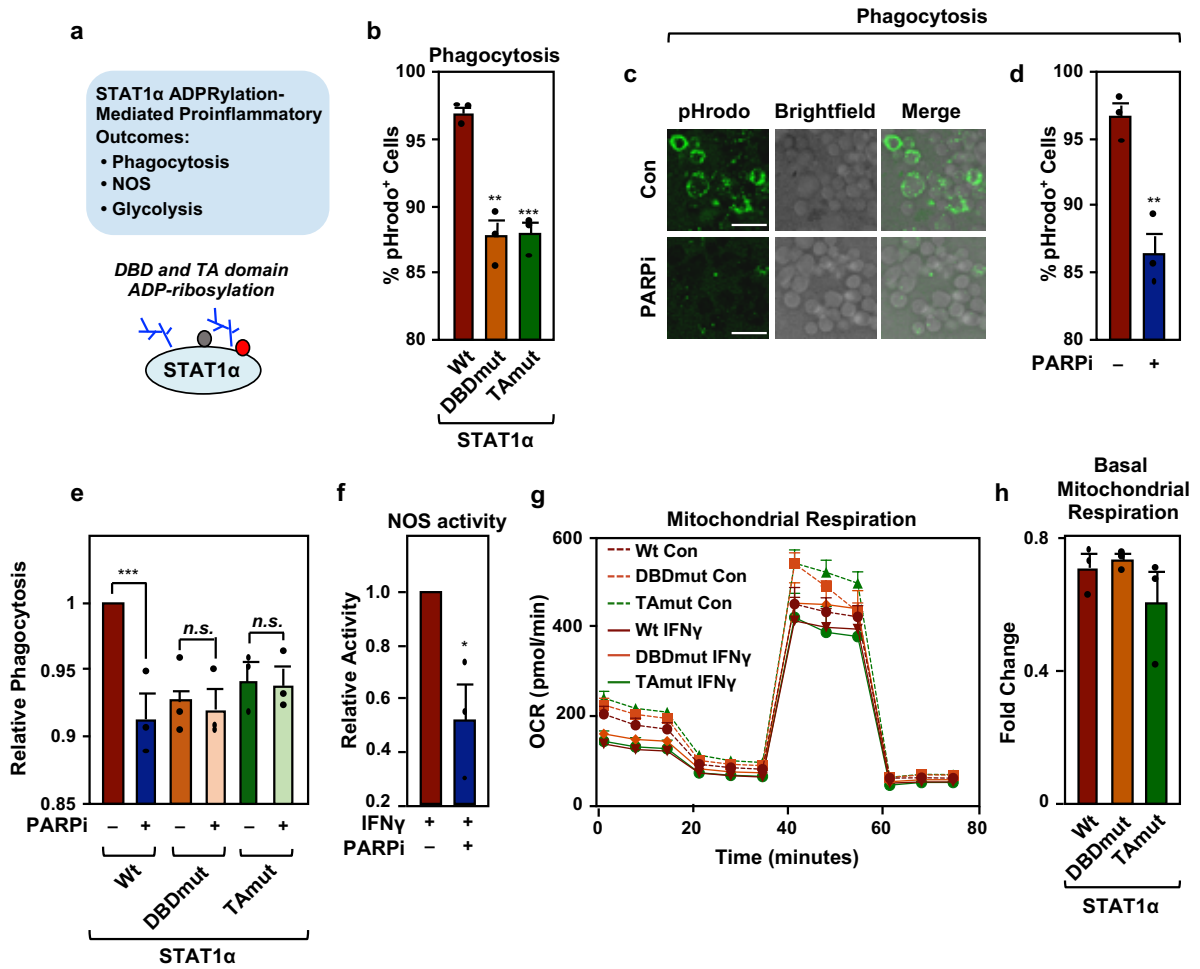
(c), (d) PARP catalytic inhibition results in reduced phagocytotic capacity in macrophages. iBMDMs were treated with PJ34 as indicated. Scale bar: 44 μ m. (d) Quantification of phagocytosis showing the number of pHrodo⁺ cells relative to the total number of cells per field for 3 independent experiments (unpaired, two-tailed Student's t-test; ** = 0.0049). Error bars represent mean \pm SEM.

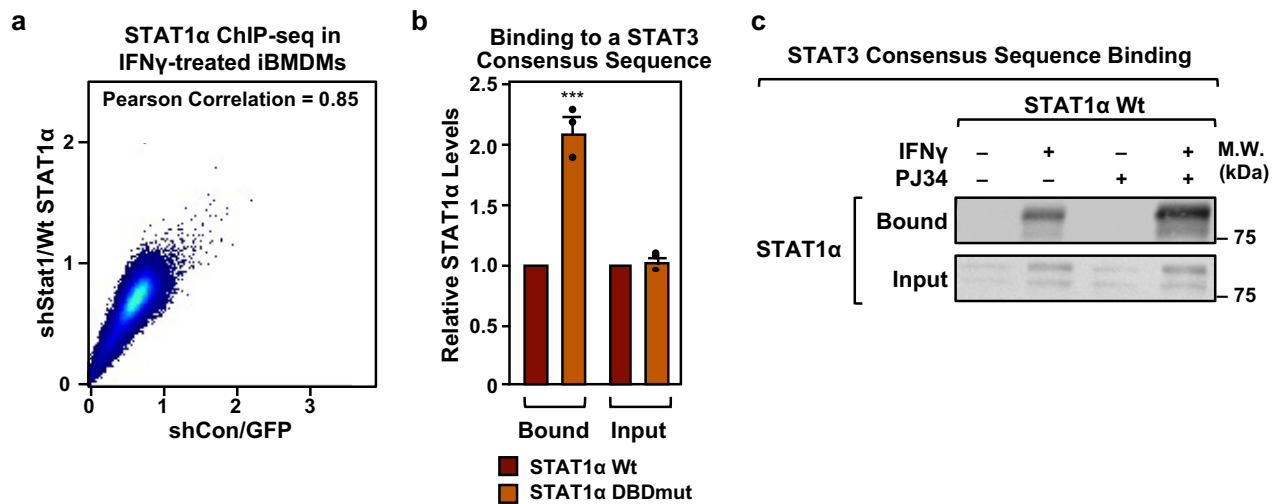
(e) PJ34 treatment does not significantly alter the relative amount of phagocytosis in iBMDMs expressing Wt or ADP-ribosylation site mutants. The p-values were determined using two-way ANOVA followed by Tukey's multiple comparison tests for 3 independent experiments (n.s., not significant at 0.05). Error bars represent mean \pm SEM.

(f) PARP catalytic inhibition results in attenuation of NOS activity in iBMDMs. The cells were treated with IFN γ and veliparib for 24 hours as indicated (n = 3; unpaired, two-tailed Student's t-test; * = 0.0132). Error bars represent mean \pm SEM.

(g), (h) ADP-ribosylation of STAT1 α does not affect mitochondrial respiration. (g) Mitochondrial respiration profile of iBMDMs expressing Wt or ADP-ribosylation site mutant (DBDmut and TAMut) STAT1 α using Seahorse assays. (h) Fold change in the level of basal mitochondrial respiration observed upon IFN γ treatment. In both panels, the assays were performed in three independent biological replicates. The significance determined using unpaired, two-tailed Student's t-test for 3 independent experiments (the results with the ADP-ribosylation site mutants of STAT1 α were not significantly different from the wild-type at p < 0.05). Error bars represent mean \pm SEM.

Supplementary Figure 8





Supplementary Figure 9. Loss of site-specific ADP-ribosylation of the STAT1 α DBD results in enhanced binding of STAT1 α to DNA.

(a) Ectopically expressed STAT1 α localizes to similar genomic loci as endogenous STAT1 α . Correlation plots comparing ChIP-seq read accumulations between iBMDMs subjected to non-specific knockdown and ectopic expression of GFP (shCon/GFP), and knockdown of endogenous STAT1 α and ectopic expression of Wt STAT1 α (shStat1/STAT1 α Wt).

(b) STAT1 α DBDmut exhibits increased binding to a STAT3 consensus sequence. Quantification of immunoblots from Fig. 5f showing the levels of STAT1 α binding under the conditions indicated (i.e., with ectopic expression of Wt or DBDmut STAT1 α and concurrent shRNA-mediated knockdown of endogenous STAT1 α). The assays were performed in three independent biological replicates. The p-values were determined using unpaired Student's t-test followed by Holm-Sidak's multiple comparison test (*** = 0.000881). Error bars represent mean \pm SEM.

(c) Inhibition of PARP-mediated ADPRylation of STAT1 α results in increased binding to a STAT3 consensus sequence. iBMDMs were treated with IFN γ \pm PJ34 as indicated. The immunoblots are representative of 3 independent experiments. Uncropped immunoblots are provided as a Source Data file.

[See Supplementary Figure 10 on the next page]

Supplementary Figure 10. Loss of site-specific ADP-ribosylation of the STAT1 α TA domain can attenuate IFN γ -stimulated phosphorylation at S727.

(a) Quantification of immunoblots from Fig. 6B showing the levels of STAT1 α S727p in iBMDMs under the conditions indicated (i.e., with ectopic expression of Wt, DBDmut, or TAmut STAT1 α and concurrent shRNA-mediated knockdown of endogenous STAT1 α). The assays were performed in three independent biological replicates. The p-values were determined using two-way ANOVA followed by Sidak's multiple comparison test (** = 0.004, n.s., not significant). Error bars represent mean \pm SEM.

(b) Immunoblots showing STAT1 α S727p in 293T transiently expressing STAT1 α Wt and ADP-ribosylation site mutants (DBDmut and TAmut). The immunoblots are representative of 3 independent experiments. Uncropped immunoblots are provided as a Source Data file.

(c) SDS-PAGE with Coomassie Blue staining showing the p300 purified from SF9 insect cells. The band corresponding to purified p300 protein is marked with a red arrow. The image is representative for one round of purification. Uncropped gel images are provided as a Source Data file.

(d) PARP-1 autoactivation attenuates its acetylation by p300. Immunoblots showing the acetylation of PARP-1 from in vitro reactions performed in the presence or absence of NAD⁺. The immunoblots are representative of 2 independent experiments. Uncropped immunoblots are provided as a Source Data file.

(e) Phosphorylation of STAT1 α on S727 is required for p300 autoacetylation. Immunoblots show autoacetylation of p300 in the presence of STAT1 α Wt or S727A mutant as indicated. The immunoblots are representative of 3 independent experiments. Uncropped immunoblots are provided as a Source Data file.

(f) Browser tracks of ChIP-seq data showing STAT1 α and H3K27ac enrichment in Wt- or TAmut-expressing iBMDMs.

(g) Heatmaps of ChIP-seq data representing the top 50% of 'maintained' STAT1 α peaks in TAmut-expressing iBMDMs compared to Wt STAT1 α -expressing iBMDMs.

Supplementary Figure 10.

